Many-body physics in the radio-frequency spectrum of lattice bosons

Kaden R. A. Hazzard* and Erich J. Mueller
Laboratory of Atomic and Solid State Physics, Cornell University, Ithaca, New York 14853
(Received 7 July 2009; revised manuscript received 22 January 2010; published 8 March 2010)

We calculate the radio-frequency spectrum of a trapped cloud of cold bosonic atoms in an optical lattice. By using random phase and local-density approximations we produce both trap-averaged and spatially resolved spectra, identifying simple features in the spectra that reveal information about both superfluidity and correlations. Our approach is exact in the deep Mott limit and in the dilute superfluid when the hopping rates for the two internal spin states are equal. It contains final state interactions, obeys the Ward identities (and the associated conservation laws), and satisfies the f-sum rule. Motivated by earlier work by Sun, Lannert, and Vishveshwara [Phys. Rev. A **79**, 043422 (2009)], we also discuss the features that arise in a spin-dependent optical lattice.

DOI: 10.1103/PhysRevA.81.033404 PACS number(s): 37.10.Jk, 32.30.Bv, 03.75.Kk, 03.75.Lm

I. INTRODUCTION

Bosonic atoms in optical lattices, described by the Bose-Hubbard model [1,2], display a nontrivial quantum phase transition between a superfluid and Mott insulator. The latter is an incompressible state with an integer number of atoms per site. In a trap, the phase diagram is revealed by the spatial structure of the gas—one has concentric superfluid and insulating shells. This structure has been elegantly explored by radio frequency (rf) spectroscopy [3], a technique that has also given insight into strongly interacting Fermi gases across the BEC-BCS crossover [4]. Here we use a random phase approximation (RPA) that treats fluctuations around the strong coupling Gutzwiller mean-field theory to explore the radio-frequency spectrum of lattice bosons.

We find two key results: (1) Our previous sum-rule-based analysis [5] of experiments at the Massachusetts Institute of Technology [3] stands up to more rigorous analysis. In the limit of small spectral shifts, the RPA calculation reduces to that simpler theory. (2) In a gas with more disparate initial- and final-state interactions (such as cesium), the spectrum becomes more complex, with a bimodal spectrum appearing even in a homogeneous gas. The bimodality reveals key features of the many-body state. For example, in the limit considered by Sun, Lannert, and Vishveshwara [6], the spectral features are related to the nearest neighbor phase coherence. In the Gutzwiller approximation, the phase coherence directly maps onto the condensate density. In this article, we provide a physical picture of this result and explain how this bimodality can be observed in a spatially resolved experiment.

A. RF spectroscopy

In rf spectroscopy, a radio wave is used to flip the hyperfine spin of an atom from $|a\rangle$ to $|b\rangle$. The rate of excitation reveals details about the many-body state because the $|a\rangle$ and $|b\rangle$ atoms have slightly different interactions. Generically, the interaction Hamiltonian is $H_{\text{int}} = \sum_j U_{aa} n_a(n_a - 1)/2 + U_{bb} n_b(n_b - 1)/2 + U_{ab} n_a n_b$, with $U_{aa} \neq U_{ab} \neq U_{bb}$, where n_σ is the number of σ-state atoms on site j. In the simplest mean-field picture, the energy needed to flip an atom on site j from state a to state b is shifted by an energy $\delta\omega = U_{bb} n_b + (U_{ab} - U_{aa}) n_a$. The application of this picture to an inhomogeneous gas suggests that the absorption spectrum reveals a histogram of the atomic density. Such a density probe is quite valuable—in addition to the aforementioned examples, it was the primary means of identifying Bose-Einstein condensation in atomic hydrogen [7].

Recently Sun, Lannert, and Vishveshwara [6] found a bimodal spectrum in a special limit of this problem, as did Ohashi, Kitaura, and Matsumoto [8] in a separate limit, calling into question this simple picture. We give a simple physical interpretation of the bimodality. As illustrated in Fig. 1, the superfluid state near the Mott insulator can be caricatured as a dilute gas of atoms or holes moving in a Mott background. An rf photon can either flip the spin of one of the core atoms or flip the spin of one of the mobile atoms. The energy of these two excitations will be very different, implying that the rf spectrum should be bimodal. Through our RPA calculation, we verify this feature, calculating the frequencies of the two peaks and their spectral weights. Interestingly, this calculation reveals that the two excitations in our cartoon are strongly hybridized.

We find that for parameters relevant to previous ^{87}Rb experiments, the degree of bimodality is vanishingly small and our previous sum-rule arguments [5] accurately describe such experiments. On the other hand, there are opportunities to study other atoms (for example, Na, Cs, and Yb) for which the bimodality may be more pronounced. Moreover, if the interactions or tunneling rates can be tuned via a spin-dependent lattice or a Feshbach resonance, then this spectral feature will appear in a dramatic fashion.

This bimodal spectrum, with one peak produced by the "Mott" component and another by the "superfluid" component, is reminiscent of the spectrum of a finite-temperature Bose gas in the absence of a lattice. As described by Oktel and Levitov [9], in that situation one sees one peak from the condensate and one from the incoherent thermal atoms. We would expect that at finite temperature our "Mott" peak continuously evolves into their "thermal" peak.

II. BOSE-HUBBARD MODEL

A. Model and rf spectra

In the rf-spectrum experiments we consider that all atoms are initially in the a-internal state and the rf pulse

*kh279@cornell.edu

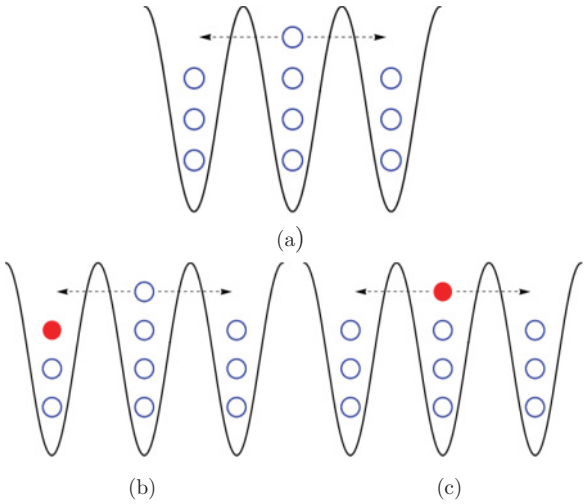

FIG. 1. (Color online) Illustration of two types of rf-active excitations of the lattice superfluid near the Mott transition. Open (blue) circles are atoms in the $|a\rangle$ state, filled (red) circles are atoms in the $|b\rangle$ state, and the arrows indicate a delocalized particle whereas other particles are localized. Panel (a) illustrates the initial superfluid state, which consists of a dilute gas of atoms moving in a Mott background. Final states in panels (b) and (c) show the excitation of a core or delocalized atom.

drives them to the b state. Consequently, we consider two-component bosons trapped in the periodic potential formed by interfering laser beams, described by a Bose-Hubbard model [1]

$$H = -\sum_{\substack{\langle i,j\rangle \\ \sigma=\{a,b\}}} t_\sigma c^\dagger_{i,\sigma} c_{j,\sigma} + \sum_{\sigma,j}(V_{j,\sigma} - \mu_\sigma) c^\dagger_{j,\sigma} c_{j,\sigma} + \sum_j \left(\sum_{\alpha,\beta} \frac{U_{\alpha\beta}}{2} c^\dagger_{j,\alpha} c^\dagger_{j,\beta} c_{j,\beta} c_{j,\alpha} \right), \quad (1)$$

where c_σ and $c^\dagger_\sigma$ are the annihilation and creation operators for states in the internal state σ, μ_σ is the chemical potential, $V_{j,\sigma}$ is the external potential with δ, the vacuum a-b splitting, absorbed into it, $U_{\alpha\beta}$ is the α-state–β-state on-site interaction strength, and t_σ is the hopping matrix element. The interactions are tunable via Feshbach resonances and spin-dependent lattices are also available [10]. For this latter setup, the hopping matrix elements may be tuned by the intensity of the lattices, and introducing small displacements of the lattice will reduce the overlap between the Wannier states of a and b atoms, and therefore may also be an efficient way to control the relative size of U_{aa} and U_{ab}. The interaction U_{bb} will be irrelevant because we will only consider the case where there is a vanishingly small concentration of b-state particles. In calculating the response to rf photons we will take $V_j =$ constant. Trap effects will later be included through a local-density approximation [5], which is valid for slowly varying traps [8,11–19].

Experimentally, the rf spectrum is measured by counting the number of atoms transferred from state a to b when the system is illuminated by an rf pulse. These dynamics are driven by a perturbation

$$H_{\rm rf} = \sum_j \gamma(t) c^\dagger_{j,b} c_{j,a} + \text{H.c.}, \quad (2)$$

where $\gamma(t)$ is proportional to the time-dependent amplitude of the applied rf field multiplied by the dipole matrix element between states a and b. Typically, γ is a sinusoidal pulse with frequency ω with a slowly varying envelope ensuring a small bandwidth. Because of the small wave number of rf photons, recoil can be neglected.

For a purely sinusoidal drive, Fermi's Golden Rule gives the number of atoms transferred per unit time for short times to be

$$\Gamma(\omega) = \frac{2\pi}{\hbar} \sum_{i,f} p_i \delta(\omega - (E_f - E_i)) |\langle f|H_{\rm rf}|i\rangle|^2, \quad (3)$$

where the sum is over the initial states (occupied with probability $p_i = e^{-\beta E_i}$) and the final states, all of which are eigenstates of H with energies E_i and E_f. We will restrict ourselves to $T = 0$ and the physically relevant case where the initial states contain no b atoms.

B. Sum rules

Taking moments of Eq. (3) [9,20,21], the mean absorbed photon frequency is

$$\langle\omega\rangle = \frac{\int d\omega \omega \Gamma(\omega)}{\int d\omega \Gamma(\omega)} = \frac{\langle [H_{\rm rf}, H] H_{\rm rf}\rangle}{\langle H^2_{\rm rf}\rangle} \quad (4)$$

$$= \delta - z(t_b - t_a) f_c + (U_{ab} - U_{aa}) g_2 \langle n\rangle. \quad (5)$$

We defined δ to be the vacuum a-b splitting, the local phase coherence factor is

$$f_c = \frac{\langle c^\dagger_{i,a} c_{j,a}\rangle}{\langle n\rangle}, \quad (6)$$

with i and j nearest neighbors, the site filling is $n \equiv c^\dagger_a c_a$, and the lattice coordination is z. The zero-distance density-density correlation function is

$$g_2 = \frac{\langle c^\dagger_a c^\dagger_a c_a c_a\rangle}{\langle n\rangle^2}. \quad (7)$$

The second term in Eq. (5) may be interpreted as the mean shift in the kinetic energy when the spin of an atom is flipped. In particular, within a strong-coupling mean-field picture $\langle c^\dagger_{i,a} c_{j,a}\rangle = \langle c^\dagger_{i,a}\rangle \langle c_{j,a}\rangle$ is the condensate density, which can therefore be measured with this technique. The second term in Eq. (5) is the shift in the interaction energy.

Our subsequent approximations will satisfy this sum rule. This is nontrivial; for example, even for the simultaneous limits of $t_b = 0$, $U_{ab} = U_{aa}$, and $t_a \to 0$ considered in Ref. [6], their results violate this sum rule by a factor of $\sim$3.

Because it plays no role in the remainder of the discussion, we will set to zero the vacuum level splitting ($\delta = 0$). This amounts to working in a "rotating frame."

III. RANDOM PHASE APPROXIMATION

A. General setup and solution

To calculate the rf spectrum, we employ a time-dependent strong-coupling mean-field theory that includes $k = 0$ fluctuations around the static strong-coupling Gutzwiller mean-field theory [2]. This mean-field theory is exact in the deep Mott limit and in the dilute superfluid when $t_a = t_b$, and it yields fairly accurate ground states in the intermediate regime [11–15]. References [8,19] previously used analogous RPA's to calculate the Bose-Hubbard model's quasiparticle spectra and rf spectra with $U_{ab} = 0$, which reduce to the $k = 0$ single-particle spectra.

We use the homogeneous time-dependent Gutzwiller variational ansatz

$$|\psi(t)\rangle = \bigotimes_i \left\{ \sum_n [f_n(t)|n, 0\rangle_i + g_n(t)|n-1, 1\rangle_i] \right\}, \quad (8)$$

where $|n_a, n_b\rangle_i$ is the state at site i with n_a particles in the a state and n_b in the b state. The equation of motion for $f_n(t)$ and $g_n(t)$ are derived by minimizing the action $S = \int dt \mathcal{L}$, with the Lagrangian

$$\mathcal{L} = \langle\psi| i\partial_t |\psi\rangle - \langle\psi|H|\psi\rangle - \lambda\langle\psi|\psi\rangle, \quad (9)$$

where λ is a Lagrange multiplier that enforces conservation of probability. At time $t = -\infty$, where $\gamma(t) = 0$, we take $g_n = 0$ and choose f_n to minimize $\langle\psi|H|\psi\rangle$:

$$\lambda f_n = -t_a z(\sqrt{n}\alpha^* f_{n-1} + \sqrt{n+1}\alpha f_{n+1}) + \left[\frac{U_{aa}}{2} n(n-1) - \mu n\right] f_n, \quad (10)$$

where

$$\alpha = \sum_n \sqrt{n} f_n^* f_{n-1}. \quad (11)$$

Upon solving the subsequent dynamics to quadratic order in γ, one finds

$$\Gamma(t) = N_s \int dt' \gamma(t)\gamma(t')\chi^{(R)}(t-t'), \quad (12)$$

where the retarded response function is

$$\chi^{(R)}(t) = \frac{1}{i} \sum_n \sqrt{n}[G_n^*(t) f_n - G_n(t) f_n^*]. \quad (13)$$

The Green's functions $G_n(t)$ satisfy the equations of motion for the g_n functions in the absence of an rf field, but in the presence of a delta-function source and for the boundary condition $G_n(t) = 0$ for $t < 0$. The relevant equations are simplest in Fourier space, where $G_n(\omega) = \int dt e^{i\omega t} G_n(t)$ obeys

$$\sqrt{n} f_n = -\omega G_n + \sum_m \Lambda_{nm} G_m, \quad (14)$$

where $\Lambda = \bar{\Lambda} + \Theta$ is a Hermitian matrix. The tridiagonal part $\bar{\Lambda}$ is

$$\bar{\Lambda}_{n,n+1} = -z t_a \alpha \sqrt{n}, \quad (15)$$

$$\bar{\Lambda}_{n,n-1} = -z t_a \alpha^* \sqrt{n-1}, \quad (16)$$

$$\bar{\Lambda}_{nn} = -\mu n - \lambda + \frac{U_{aa}}{2}(n-1)(n-2) + U_{ab}(n-1). \quad (17)$$

The remaining contribution Θ is

$$\Theta_{nm} = -z t_b f_{n-1} f_{m-1}^*. \quad (18)$$

Specializing to the case where $\gamma(t) = \gamma e^{i\omega t}$, the response is given in terms of normalized eigenvectors v_m, with $\sum_m \Lambda_{nm} v_m^{(j)} = \epsilon_j v_n^{(j)}$. It takes the form of a sum of delta functions:

$$I(\omega) = \sum_j \left(\sum_m \sqrt{m} f_m v_m^{(j)} \right)^2 \delta(\omega - \epsilon_j). \quad (19)$$

The f_n are found at each point in the phase diagram by starting with a trial α, solving Eq. (10), then updating α via Eq. (11) and iterating. We find that almost all spectral weight typically lies in only one or two peaks. Figure 2 shows sample spectra, whose general behavior is discussed in more detail in Sec. III B. The superfluid near the Mott state displays a multimodal spectrum, but in the weakly interacting limit only a single peak is seen. An avoided crossing is clearly visible in these plots. Taking moments of $\chi^R(\omega)$, we see that Eq. (5) is satisfied.

B. Limiting cases and dependence on final-state interactions

1. *Evolution of bimodality over the phase diagram*

Although finding the spectrum in Eq. (19) is a trivial numerical task, one can gain further insight by considering limiting cases. First, when $U_{ab} = U_{aa}$ and $t_a = t_b$, the system possesses an SU(2) symmetry. In this limit we find that $G_n(t) = -i\sqrt{n} f_n \theta(t)$ is constant for $t > 0$. Thus our approximation gives a spectrum $I(\omega)$ that is proportional to $\delta(\omega)$. This result coincides with the exact behavior of the system; the operator $X = \sum_j b_j^\dagger a_j$ is a ladder operator, $[H, X] = \delta X$, and it can only generate excitations with energy δ (set equal to zero in our calculation). The fact that our approximations correctly capture this behavior is nontrivial—in a field theoretic language one would say that our equation of motion approach includes the vertex corrections necessary for satisfying the relevant "Ward identities" [22–24].

The current ^{87}Rb experiments are slightly perturbed from this limit, with $(U_{ab} - U_{aa})/U_{aa} \approx -0.024$ and $t_b = t_a$. We find that the δ function is shifted by a frequency proportional to $U_{ab} - U_{aa}$, but that the total spectral weight remains concentrated on that one frequency. The sum of the spectral weights at all other frequencies scale as $\eta \equiv (U_{ab} - U_{aa})/(z t_a)$. Consequently, it is an excellent approximation to treat the spectrum as a delta function, and our RPA calculation reduces to the results in Ref. [5]. We emphasize, however, that other atoms, such as cesium, can be in a regime where η is large.

When $\eta \ll 1$ [that is, rapid tunneling rates $t_a \gg (U_{ab} - U_{aa})/z$] the spectral weight is concentrated in a single, shifted peak. Conversely, when $\eta \gg 1$ [that is, slow tunneling rates $t_a \ll (U_{ab} - U_{aa})/z$], the spectral weight is generically multimodal. This behavior can be understood as an analog of

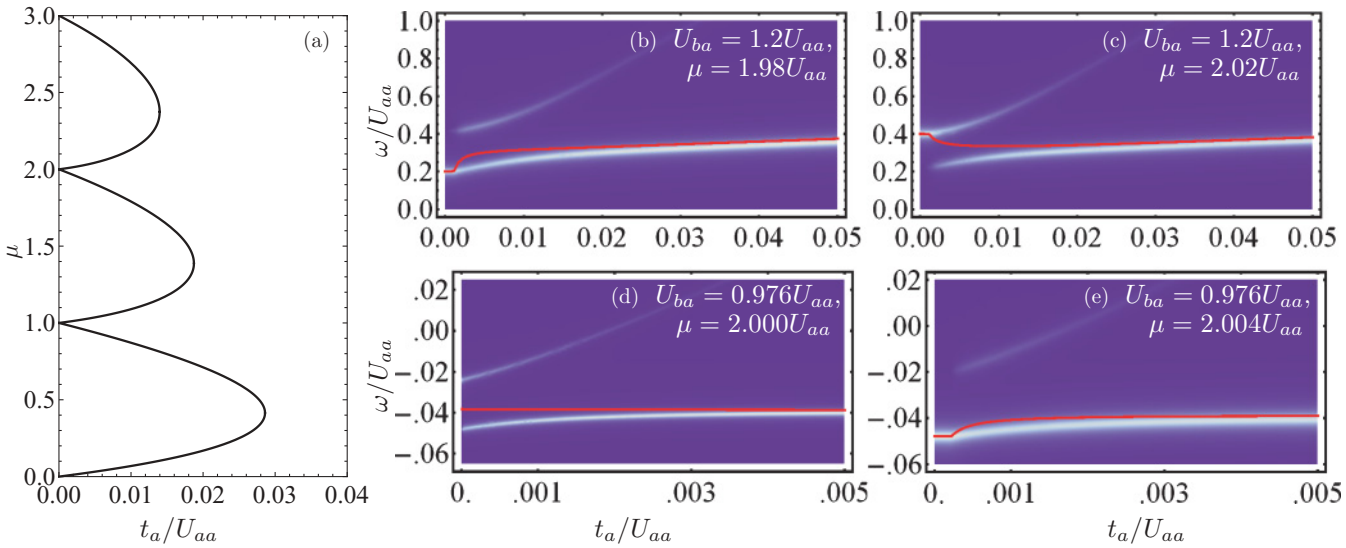

FIG. 2. (Color online) Spectral density of a homogeneous system as a function of ω/U_{aa} and t_a/U_{aa} (whiter regions indicate larger spectral density) compared with sum-rule prediction (red line). Delta functions are broadened to Lorentzians for visualization purposes. (a) Ground state phase diagram within the Gutzwiller approximation, for reference. In panels (b) and (c), we take $U_{ba} = 1.2U_{aa}$ and $t_b = t_a$, with (b) $\mu = 1.98U_{aa}$ and (c) $\mu = 2.02U_{aa}$. In panels (d) and (e), we take parameters corresponding to typical ^{87}Rb experiments, $U_{ba} = 0.976U_{aa}$ and $t_b = t_a$, and take (d) $\mu = 2.000U_{aa}$ and (e) $\mu = 2.004U_{aa}$. In both cases, a double-peak structure is visible, but the region of the phase diagram in which it is important is much smaller for ^{87}Rb parameters than for the parameters for panels (b) and (c).

"motional narrowing" [25]. Our cartoon in Fig. 1 gives two excitation processes, and the two states can convert between themselves at a rate $\sim z t_a$. One will only be to separately resolve the two states if the splitting between them is large compared to the rate of the interconversion.

2. *Analytic solution in deep-lattice limit*

We gain further insight by considering the superfluid near the Mott phase with $t_a/U_a \ll 1$. Here, one can truncate the basis to two states with total particle number n and $n+1$ on each site. In this truncation, our calculation is the mean-field implementation of the picture in Fig. 1. Then the f_n and G_n can be found analytically; one only needs to solve 2×2 linear algebra problems. In the limit $t_b = 0$ and $U_{ab} = U_{aa}$, this is similar to the approach of Ref. [6], but it includes the hopping self-consistently, allowing us to satisfy the sum rule (5). This truncation is exact in the small-t_a limit, and yields

$$\chi^{(R)}(\omega) = A_+ \delta(\omega - \omega_+) + A_- \delta(\omega - \omega_-), \tag{20}$$

with

$$\omega_\pm = \frac{\epsilon_1 + \epsilon_2}{2} \pm \sqrt{\Delta^2 + \left(\frac{\epsilon_1 - \epsilon_2}{2}\right)^2}, \tag{21}$$

where

$$\begin{aligned} \epsilon_1 &\equiv (U_{ab} - U_{aa})(n-1) + z t_a f_{n+1}^2 (n+1) \\ \epsilon_2 &\equiv (U_{ab} - U_{aa}) n + z[t_a(n+1) - t_b] f_n^2 \\ \Delta &\equiv -\sqrt{n(n+1)}\, t_a z f_n f_{n+1} \end{aligned} \tag{22}$$

if $n \geqslant 1$, and

$$\begin{aligned} \epsilon_1 &\equiv z t_a f_1^2 \\ \epsilon_2 &\equiv z(t_a - t_b) f_0^2 \\ \Delta &\equiv 0 \end{aligned} \tag{23}$$

if $n = 0$ (here, only the ϵ_2 peak has nonzero spectral weight). We omit the cumbersome analytic expressions for the spectral weights $A_\pm$. The spectrum consist of two peaks—hybridized versions of the excitations caricatured in Fig. 1. One can identify ϵ_1 and ϵ_2 as the energies of those caricature processes, recognizing that the hybridization term Δ grows with t_a. The avoided crossing between these modes is evident in Fig. 2.

C. Inhomogeneous spectrum

We model the trapped spectrum through a local-density approximation. We assume that a given point in the trap has the properties of a homogeneous gas with chemical potential $\mu(r) = \mu_0 - V(r)$. In Fig. 3, we show the density profile and the spectrum corresponding to each point in space. Also shown is the trap-averaged spectrum.

When U_{ab} is slightly smaller than U_{aa}, corresponding to ^{87}Rb and illustrated in Fig. 3(e), the spectrum is unimodal at each point in space. The shift, given by the sum rule in Eq. (5), maps out the density seen in Fig. 3(a). For larger $|U_{ab} - U_{aa}|$, illustrated in Fig. 3(b), the spectrum in the superfluid regions is distinctly bimodal. If, as in Fig. 3(c), one makes $U_{ab} = U_{aa}$ but sets $t_b \neq t_a$, the spectrum reflects the condensate density rather than the particle density. One only sees spectral shifts in the superfluid regions—spectral weight gradually shifts from one peak to another as one moves in space. In Fig. 3(d),

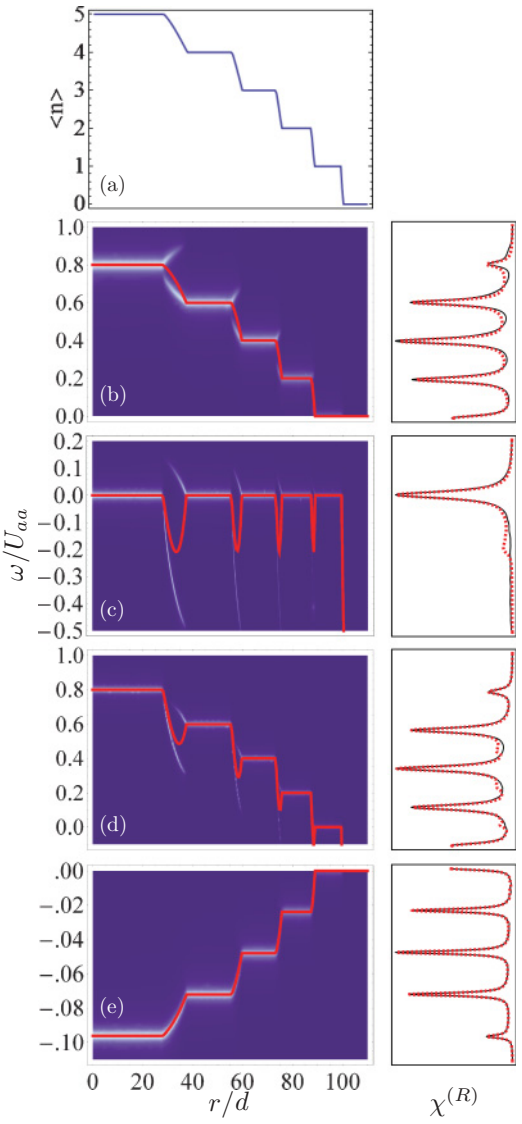

FIG. 3. (Color online) (a) Density n as a function of distance to trap center rescaled by the lattice spacing r/d in a local-density approximation. For all subfigures, we take $t_a/U_{aa} = 0.004$, which is moderately smaller than the tip of the first Mott lobe. The left side of panels (b) to (e) show the spectrum of a homogeneous gas with density $n(r)$, representing the spatially resolved spectrum observed in an experiment on a trapped gas. The horizontal axis is position, the vertical axis is frequency, and the color from dark to light represents increasing spectral density. The continuous (red) curve denotes the sum-rule result for $\langle\omega\rangle$. We round the δ-functions to Lorentzians for visualization. The right side of panels (b) to (e) shows the trap-averaged spectrum for a three-dimensional trap within our RPA (black, solid line) compared with the sum rule (red, dashed line). (b) $U_{ab} = 1.2U_{aa}$, $t_b = t_a$; (c) $U_{ab} = U_{aa}$, $t_b = t_a + 0.1U_{aa}$; (d) $U_{ab} = 1.2U_{aa}$, $t_b = t_a + 0.1U_{aa}$; (e) ^{87}Rb parameters: $U_{ab} = 0.976U_{aa}$, $t_b = t_a$.

we illustrate what happens when both $U_{ab} \neq U_{aa}$ and $t_b \neq t_a$. One sees a pattern that is roughly a superposition of Figs. 3(b) and 3(c).

In all cases, the bimodality of the homogeneous spectrum is quite effectively washed out by the inhomogeneous broadening of the trap. On the other hand, if one spatially images the atoms flipped into the b state as in Ref. [3], there is a clear qualitative signature of the bimodality. If one excites the system with an rf pulse whose frequency lies between the resonant frequencies of two Mott plateaus, one will excite two "shells" of atoms. These shells should be clearly visible, even in column-integrated data.

IV. CONCLUSIONS AND DISCUSSION

In this article, we have shown that the rf spectra of a homogeneous Bose gas in an optical lattice will have two (or more) peaks in the superfluid state when the parameters are tuned close to the superfluid Mott-insulator phase transition. Physically, this bimodality is a result of the strong correlations in the system. These correlations result in two distinct forms of excitations (which are strongly hybridized): those involving "core" atoms and those involving delocalized atoms. When $\eta = (U_{ab} - U_{aa})/(zt_{aa})$ is small, such as in typical ^{87}Rb experiments, this bimodality is absent.

Our approach, based upon applying linear response to a time-dependent Gutzwiller mean-field theory, is both simple and quite general. It allows arbitrary interactions between both spin states, and it allows arbitrary spin-dependent hopping rates. The major weakness of the theory is that it fails to fully account for short-range correlations—the atoms are in a quantum superposition of being completely delocalized and confined to a single site. The physical significance of this approximation is most clearly seen when one considers the case where the final-state atoms have no interactions (i.e., $U_{ab} = 0$) and see no trap or lattice. Imaging the b atoms after a time of flight is analogous to momentum-resolved photoemission [26] and would reveal the dispersion relationship of the single-particle excitations. The fact that the spectrum consists of two sharp peaks means that all of the noncondensed atoms are approximated to have the same energy. One will also see that their momentum is uniformly distributed throughout the first Brillioun zone. In the strong-lattice limit, where the bandwidth is small, this approximation is not severe.

ACKNOWLEDGMENTS

We thank Sourish Basu, Stefan Baur, Stefan Natu, Eliot Kapit, Wolfgang Ketterle, Kuei Sun, Smitha Vishveshwara, Henk Stoof, Ian Spielman, and Mukund Vengalattore for useful discussions. This material is based upon work supported by the National Science Foundation through Grant No. PHY-0758104 and was performed partially at the Aspen Center for Physics.

[1] D. Jaksch, C. Bruder, J. I. Cirac, C. W. Gardiner, and P. Zoller, Phys. Rev. Lett. **81**, 3108 (1998).

[2] M. P. A. Fisher, P. B. Weichman, G. Grinstein, and D. S. Fisher, Phys. Rev. B **40**, 546 (1989).

[3] G. K. Campbell, J. Mun, M. Boyd, P. Medley, A. E. Leanhardt, L. G. Marcassa, D. E. Pritchard, and W. Ketterle, Science **313**, 649 (2006).
[4] I. Bloch, J. Dalibard, and W. Zwerger, Rev. Mod. Phys. **80**, 885 (2008).
[5] K. R. A. Hazzard and E. J. Mueller, Phys. Rev. A **76**, 063612 (2007).
[6] K. Sun, C. Lannert, and S. Vishveshwara, Phys. Rev. A **79**, 043422 (2009).
[7] D. G. Fried, T. C. Killian, L. Willmann, D. Landhuis, S. C. Moss, D. Kleppner, and T. J. Greytak, Phys. Rev. Lett. **81**, 3811 (1998).
[8] Y. Ohashi, M. Kitaura, and H. Matsumoto, Phys. Rev. A **73**, 033617 (2006).
[9] M. O. Oktel and L. S. Levitov, Phys. Rev. Lett. **83**, 6 (1999).
[10] I. H. Deutsch and P. S. Jessen, Phys. Rev. A **57**, 1972 (1998).
[11] L. Pollet, S. Rombouts, K. Heyde, and J. Dukelsky, Phys. Rev. A **69**, 043601 (2004).
[12] S. Bergkvist, P. Henelius, and A. Rosengren, Phys. Rev. A **70**, 053601 (2004).
[13] S. Wessel, F. Alet, M. Troyer, and G. G. Batrouni, Phys. Rev. A **70**, 053615 (2004).
[14] G. G. Batrouni, V. Rousseau, R. T. Scalettar, M. Rigol, A. Muramatsu, P. J. H. Denteneer, and M. Troyer, Phys. Rev. Lett. **89**, 117203 (2002).
[15] B. DeMarco, C. Lannert, S. Vishveshwara, and T.-C. Wei, Phys. Rev. A **71**, 063601 (2005).
[16] N. Dupuis and K. Sengupta, Physica B: Condensed Matter **404**, 517 (2009).
[17] K. Sengupta and N. Dupuis, Phys. Rev. A **71**, 033629 (2005).
[18] S. Konabe, T. Nikuni, and M. Nakamura, Phys. Rev. A **73**, 033621 (2006).
[19] C. Menotti and N. Trivedi, Phys. Rev. B **77**, 235120 (2008).
[20] M. O. Oktel, T. C. Killian, D. Kleppner, and L. S. Levitov, Phys. Rev. A **65**, 033617 (2002).
[21] M. O. Oktel and L. S. Levitov, Phys. Rev. Lett. **83**, 6 (1999).
[22] C. J. Pethick and H. T. C. Stoof, Phys. Rev. A **64**, 013618 (2001).
[23] G. Baym, Phys. Rev. **127**, 1391 (1962).
[24] J. Zinn-Justin, *Quantum Field Theory and Critical Phenomena* (Oxford University Press, New York, 2002).
[25] C. P. Slichter, in *Principles of Magnetic Resonance*, edited by D.-I. H. K. V. Lotsch (Springer-Verlag, New York, 1990).
[26] J. T. Stewart, J. P. Gaebler, and D. S. Jin, Nature (London) **454**, 744 (2008).